Mobile qubits in quantum Josephson circuits

Toshiyuki Fujii,[1] Munehiro Nishida,[2] and Noriyuki Hatakenaka[1]
[1]*Graduate School of Integrated Arts and Sciences, Hiroshima University, Higashi-Hiroshima 739-8521, Japan*
[2]*Graduate School of Advanced Sciences of Matter, Hiroshima University, Higashi-Hiroshima 739-8530, Japan*
(Received 14 September 2007; published 10 January 2008)

A massive mobile qubit is proposed that uses quantum-mechanical aspects of a *mobile bound excitation pair* consisting of a fluxon and an antifluxon, called a breather, in a long Josephson junction with small capacitance per unit length. This massive mobile qubit acts as a quantum data bus that transfers quantum information from one node to another. Moreover, it performs calculations during communication without the support of stationary qubits. In addition, the proposed qubits are elementary excitations that are regarded as macroscopic artificial two-level atoms. This means they can be introduced anytime and anywhere on demand in contrast to built-in solid-state qubits. They provide a platform for testing fundamental problems in quantum mechanics on a macroscopic scale.

DOI: 10.1103/PhysRevB.77.024505 PACS number(s): 85.25.Cp, 03.67.Lx, 74.50.+r

I. INTRODUCTION

The transfer of quantum states from one place to another is at the heart of many quantum-information processing systems such as quantum computers and quantum communication systems. Of the various qubits that have been implemented,[1–3] solid-state qubits are especially interesting because of their potential suitability for integration. A superconducting circuit including Josephson junctions is a particularly promising candidate because of its relatively long decoherence time of $1-5$ μs.[4,5] Most studies thus far have focused on Josephson qubits in charge and flux domains, reflecting the Heisenberg uncertainty relation between the numbers of excess Cooper pairs n and the phase difference ϕ across the junction.

In these Josephson qubits with strong constant interqubit coupling, it is easy to create the entangled states that are essential for quantum-information processing. However, this constant coupling can have an undesirable effect on the implementation of quantum logic gates, for example, it appears to be difficult to manipulate only one qubit and leave the other unaffected. In general, solid-state based qubits are incorporated in solid-state elements with *always-on* coupling. Therefore, special technique is needed to perform qubit operations for each single qubit or a pair of qubits without influencing the remaining qubits. Moreover, the precise mechanism of this qubit interaction has remained unresolved.

Controllable interqubit coupling via external fields has already been investigated for charge and phase qubits.[6,7] The strength of these coupling schemes can be controlled in the time domain; i.e., the coupling of *a given pair of qubits* can be switched on and off on demand. However, this coupling cannot be controlled in the spatial domain, i.e., interacting qubit pairs are predetermined by the qubit arrangement, and perfect decoupling seems difficult to achieve, especially in large integrated qubit registers.

Another possible solution to this qubit interaction problem is based on converting a "stationary qubit" to a "mobile qubit," namely, a mobile bit of quantum information. A mobile qubit can control the coupling in the spatial domain by changing the distance between two interacting qubits. Generally, the separation distance increases as the interaction between qubits becomes weaker. Therefore, in practice, the interaction can be switched off by realizing a large separation between the qubits. A noteworthy feature of the mobile qubit is that it is capable of replacing one of the interacting qubits. Moreover, the control of the relative speed of a pair of qubits makes it possible to control the interaction time. Thus, the mobile nature of the qubit enables us to control the interqubit coupling in both the time and spatial domains.

The mobile qubit has already been implemented in both optical systems[8] and cavity QEDs.[9] Although the optical qubit has an advantage as regards maintaining its coherence, a two-qubit gate is difficult to achieve owing to the weak interaction between the photons. In addition, an optical qubit cannot change its speed. Thus, the interaction time or the degree of the phase shift is predetermined by the design of the gate as regards such factors as the quality of the nonlinearity of Kerr media. Therefore, a mobile qubit with controllable interqubit coupling and speed is an additional advantage in terms of designing a universal quantum computer. In this paper, we propose a type of flux qubit, i.e., a mobile qubit, using *elementary excitations*, known as breathers in superconducting solid-state quantum circuits. This mobile qubit in the solid state can interact stronger than an optical qubit.

II. JOSEPHSON BREATHER QUBIT

A. Classical fluxons

The dynamics of the phase difference across a long Josephson junction (LJJ) in the presence of dissipation and external forces obeys the perturbed sine-Gordon equation,

$$\phi_{tt} - \phi_{xx} + \sin\phi = \mathcal{F}, \tag{1}$$

where $\phi_t \equiv \partial\phi/\partial t$ and $\phi_x \equiv \partial\phi/\partial x$. The spatial coordinate x and the time t are normalized by the Josephson penetration depth λ_J and the inverse Josephson plasma frequency ω_J^{-1}, respectively. The perturbation term describes the effect of the bias current and the dissipation, and it is represented as $\mathcal{F}$

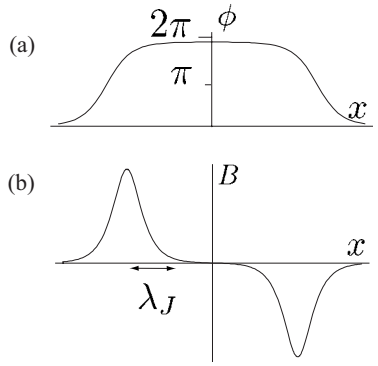

FIG. 1. A schematic of a breather: a fluxon and an antifluxon bound pair. (a) Josephson phase difference along the line and (b) magnetic flux density.

$=\varepsilon-\alpha\phi_t$, where $\varepsilon=j_b/j_c$ with j_b and j_c being the bias current density and the Josephson critical current density, respectively. The damping factor due to dissipative quasiparticle tunneling is defined as $\alpha=(\omega_J CR)^{-1}$, where C and R are the junction capacitance and resistance, respectively. The sine-Gordon equation ($\mathcal{F}=0$) has a localized wave solution (soliton) expressed in its moving frame as

$$\phi = 4\tan^{-1} e^{\pm x}, \tag{2}$$

where the plus and the minus signs correspond to a fluxon and an antifluxon with a quantum unit of magnetic flux $h/2e$. Since fluxons can carry one bit of information, classical fluxon dynamics has been studied in terms of such applications as Josephson computing[10] and rapid single-flux-quantum devices.[11] However, there is little information available about the quantum behavior of fluxons.[12–14]

Recently, the quantum behavior of fluxons has been successfully demonstrated in an annular Josephson junction under an external magnetic field.[15,16] Wallraff *et al.* observed the quantum decay of a fluxon from a metastable state by finding temperature independent escape processes using switching current distribution analysis. They also observed quantized energy levels in the potential. Their experiments opened a new pathway toward quantum computation. In fact, they proposed a new type of qubit that uses a fluxon in a long heart-shaped Josephson junction.[17] However, their fluxon qubit is constructed by the superposition of spatially distinct macroscopic quantum states. Thus, it is still a stationary qubit, meaning that it presents the same difficulties as existing flux qubits.

We can consider a simple extension of the flux qubit in superconducting quantum interference devices to a fluxon qubit in LJJs. However, in principle, we are unlikely to realize the superposition of the fluxon and antifluxon states. This is because there are no bounce solutions between the fluxons and antifluxons due to the tunneling in a (1+1) dimensional scalar field as suggested by Derrick's theorem.[18]

An alternative way to construct fluxon qubits is to use a breather (see Fig. 1), which is regarded as a bound state of a fluxon and an antifluxon in LJJs expressed as

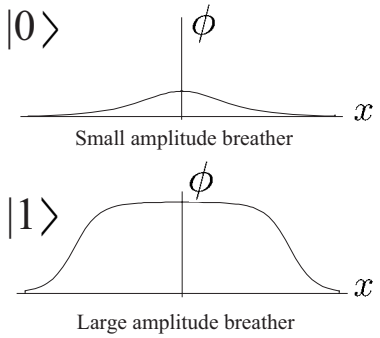

FIG. 2. A schematic of a breather qubit. The qubit basis is composed of two different energy states of the breather.

$$\phi_B = 4\tan^{-1}\left(\frac{k}{\omega_B}\frac{\sin\omega_B t}{\cosh kx}\right), \tag{3}$$

where $k=\sqrt{1-\omega_B^2}$ and ω_B is the breather internal frequency.

B. Quantum breathers

When the junction capacitance per unit length in LJJs becomes small, the breather's internal frequency is quantized. According to the Bohr-Sommerfeld quantization rule, the breather's energy E_B is then quantized as follows:[19,20]

$$E_B = 16E_J \sin\left[\frac{\hbar\omega_J}{16E_J}\left(n+\frac{1}{2}\right)\right], \quad n=0,1,2,\ldots, \tag{4}$$

where $E_J=\varepsilon_J\lambda_J W$ is the specific energy of the junction with ε_J and W being the Josephson coupling energy per unit area and the junction width, respectively. This relation holds only when the sinusoidal function argument is less than $\pi/2$. Outside this range, a breather dissociates into a fluxon and an antifluxon. Note that the energy levels are not *equidistant*. The lowest two levels thus serve as a qubit. Figure 2 shows a schematic diagram of a qubit using such a quantized breather. The qubit information is assigned to the amplitude of the breather. The number of levels is roughly determined by the ratio $q=E_J/\hbar\omega_J$. Only two energy levels required for a qubit exist when the ratio satisfies the relation $3/16\pi < q \leqslant 5/16\pi$, so the quantum breather could be regarded as a *macroscopic two-level atom* that acts as a qubit.

However, the rate q is too large to satisfy this condition in existing junctions. The junction parameters are assumed to be a junction thickness d of 2 nm, a junction width W of 20 nm, a London penetration depth λ_L of 600 nm for NbN electrodes,[21] and a relative permittivity ϵ_r of 9.65 for the MgO insulating layer.[22] These yield $q=3.4$, and the number of energy levels is $N_0 \cong 8\pi q=87$. Thus, conventional Josephson breathers contain many internal levels. In such a case, the breather energy given by Eq. (4) is reduced to $E_B=\hbar\omega_J(n+1/2)$ for a large q. The breather behaves like a plasmon in the system and no longer appears to be a qubit.

To reduce the number of energy levels, we employ the same technique for a phase qubit in a current-biased Josephson junction, i.e., we introduce a bias current. When $\varepsilon \neq 0$, Eq. (1) no longer has an analytical solution. Here, we employ

a collective-coordinate approach[23] to estimate the number of levels under the current bias. With this approach, a breather is described as the summation of a fluxon and an antifluxon, and then its dynamics is characterized by a collective coordinate $r(t)$ that is the separation between a fluxon and an antifluxon at time t,

$$\phi[x,r(t)] = 4\tan^{-1} e^{\Gamma[x+r(t)/2]} - 4\tan^{-1} e^{\Gamma[x-r(t)/2]} = 4\tan^{-1}\left(\frac{\sinh \Gamma r(t)/2}{\cosh \Gamma x}\right). \quad (5)$$

The parameter Γ indicates the inverse width of a fluxon and varies from 0 to 1 as the breather's energy increases in the absence of a bias current. Substituting Eq. (5) into the sine-Gordon Lagrangian,

$$L = \int \mathcal{L}(\phi, \phi_x, \phi_t)dx = E_J \int dx\left(\frac{1}{2}(\phi_t^2 - \phi_x^2) - (1 - \cos\phi) + \varepsilon\phi\right), \quad (6)$$

we obtain a one-particle Lagrangian,

$$L = E_J\left(\frac{m(r)}{2}\dot{r}^2 - V(r) - V_{ex}(r)\right), \quad (7)$$

and the corresponding Hamiltonian,

$$H = E_J\left(\frac{p^2}{2m(r)} + V(r) + V_{ex}(r)\right), \quad (8)$$

where

$$V(r) = 8\Gamma\left(1 - \frac{\Gamma r}{\sinh \Gamma r}\right) + \frac{8}{\Gamma}\tanh^2\frac{\Gamma r}{2}\left(1 + \frac{\Gamma r}{\sinh \Gamma r}\right), \quad (9)$$

$$V_{ex}(r) = -2\pi\varepsilon r, \quad (10)$$

and $\dot{r} = dr/dt$. The particle mass $m(r)$ is given by

$$m(r) = 4\Gamma\left(1 + \frac{\Gamma r}{\sinh \Gamma r}\right). \quad (11)$$

The Euler-Lagrange equation for r is

$$\frac{d}{dt}\left(\frac{\partial L}{\partial \dot{r}}\right) - \frac{\partial L}{\partial r} = 0. \quad (12)$$

For $\varepsilon = 0$, this approach with ansatz function (5) reproduces an exact breather solution.[24]

By using the Bohr-Sommerfeld quantization rule,

$$S(E_n) = 2q\hbar\int_{r_l}^{r_r} dr\sqrt{2m(r)[E_n - U(r)]} = 2\pi\hbar\left(n + \frac{1}{2}\right), \quad (13)$$

with $U(r) = V(r) + V_{ex}(r)$, where r_r and r_l indicate classical turning points of $U(r)$. The total number of levels in the well is approximately given by

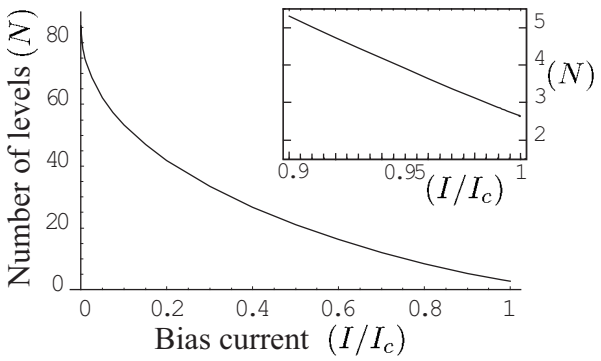

FIG. 3. The number of breather energy levels as a function of bias current.

$$N = S(U_M)/2\pi\hbar, \quad (14)$$

where U_M is the height of the potential barrier. The numerical results are shown in Fig. 3. The number of levels decreases monotonically from the unbiased value of 87, and it achieves $N \sim 3$ at $\varepsilon = 0.95$ and $N \sim 2$ at $\varepsilon = 0.97$. In our calculations, Γ was set to 1 for simplicity. As a result, we obtained a two-level quantum breather under a bias slightly below the Josephson critical current that is similar to a Josephson phase qubit. The separation of the two lowest levels is roughly estimated with a cubic potential approximation as

$$\omega_{01} \simeq \omega_0\left(1 - \frac{5}{36}\frac{\hbar\omega_0}{U_M}\right) \quad (15)$$

and

$$\omega_{12} \simeq \omega_0\left(1 - \frac{5}{18}\frac{\hbar\omega_0}{U_M}\right), \quad (16)$$

when the ratio of the frequency ω_0 at the bottom of the potential and the potential height U_M is given as $U_M/\hbar\omega_0 \sim 2.8$ at $\varepsilon = 0.95$. The transition frequency between qubit states is $\omega_{01} \simeq 0.95\omega_0$, and the separation of the two lowest resonant frequencies is sufficient to distinguish them since $\omega_{01} - \omega_{12} \simeq 0.053\omega_{01}$, which is the same as the phase qubit value. Thus, the biased breather serves as a qubit (see Fig. 4).

III. QUANTUM LOGIC GATES

Let us consider the quantum logic gates required for a quantum computer. Any quantum algorithm, namely, any unitary operation in the Hilbert space of n qubits, can be

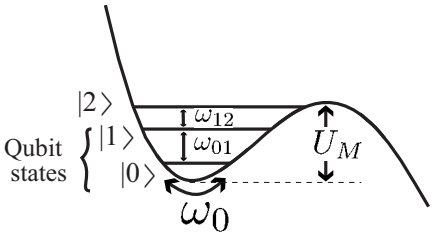

FIG. 4. Qubit states

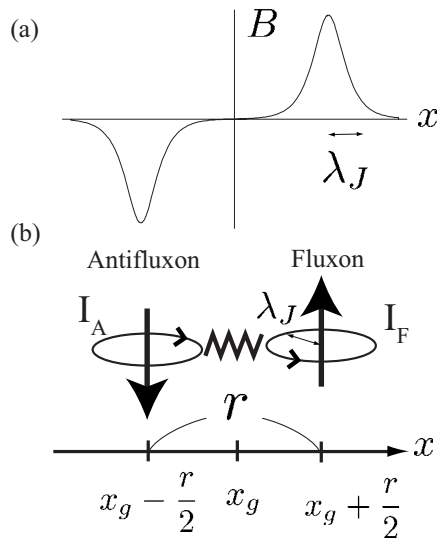

FIG. 5. Schematic of a breather: a fluxon and an antifluxon bound pair. (a) Magnetic flux density and (b) coupled circuit model of a breather.

decomposed into one-qubit unitary gates and two-qubit universal gates such as controlled-NOT (CNOT) gates.[25] In this section, we demonstrate the way in which these elementary gates are composed of Josephson breather qubits.

A. One-qubit operation

Let us assume an interaction between a quantum breather and a stationary alternating-current (ac) circuit. The breather is modeled as a coupled fluxon and antifluxon with a distance r, as shown in Fig. 5. In addition, the fluxon (antifluxon) is assumed to be composed of a circulating supercurrent I_F ($I_A=-I_F$) of radius λ_J. The circulating current is estimated by combining the following two relations. The magnetic flux density in the center of the ring produced by the circulating current I_F is expressed as $B_I=\mu I_F/2\lambda_J$, where μ is the magnetic permeability of the insulator. On the other hand, the Josephson relation leads to $B_F=(\hbar/2el)\cdot\partial\phi/\partial x|_{x=0}=\hbar/el\lambda_J$, where l is the effective thickness of the junction expressed as $l=2\lambda_L+d$. The circulating supercurrent I_F then yields $I_F=2\hbar/\mu el$ by setting $B_I=B_F$. The interaction Hamiltonian between the ac circuit and the breather located at a coordinate x_g is written as follows:

$$\begin{aligned} H_1 &= I_{ac}(t)[M(x_F)I_F + M(x_A)I_A] \\ &= I_{ac}(t)I_F\left[M\left(x_g+\frac{r}{2}\right) - M\left(x_g-\frac{r}{2}\right)\right] \\ &\simeq I_{ac}(t)I_F\frac{dM(x_g)}{dx}r, \end{aligned} \tag{17}$$

where $M(x)$ is the mutual inductance between an ac circuit and the fluxon at position x on the line. Here, $x_{F(A)}=x_g+(-)r/2$ is the position of the fluxon (antifluxon).

In the quantum-mechanical regime, the collective coordinate r is replaced by the operator $\hat{r}$. In terms of the qubit bases $|0\rangle$ and $|1\rangle$, the operator $\hat{r}$ is represented as

$$\begin{aligned} \hat{r} &= \left\{\sum_{i=0}^{1}|i\rangle\langle i|\right\}\hat{r}\left\{\sum_{j=0}^{1}|j\rangle\langle j|\right\} = \frac{r_{11}-r_{00}}{2}(|1\rangle\langle 1| - |0\rangle\langle 0|) \\ &+ r_{01}(|1\rangle\langle 0| + |0\rangle\langle 1|) + \frac{r_{11}+r_{00}}{2}(|1\rangle\langle 1| + |0\rangle\langle 0|), \end{aligned} \tag{18}$$

where $r_{ij}=\langle i|\hat{r}|j\rangle$. Using Pauli operators $\hat{\sigma}_{x,y,z}$, $\hat{r}$ is represented as

$$\hat{r} = Z\hat{\sigma}_z + X\hat{\sigma}_x, \tag{19}$$

where

$$\begin{aligned} Z &= \frac{1}{2}(\langle 1|\hat{r}|1\rangle - \langle 0|\hat{r}|0\rangle) = \frac{-1}{4\pi E_J}\left(\langle 1|\frac{\partial\hat{H}}{\partial\varepsilon}|1\rangle - \langle 0|\frac{\partial\hat{H}}{\partial\varepsilon}|0\rangle\right) \\ &= \frac{-1}{4\pi E_J}\frac{\partial}{\partial\varepsilon}(E_1 - E_0) = -\frac{\hbar\omega_J}{4\pi E_J}\frac{\partial\omega_{01}}{\partial\varepsilon} = -\frac{1}{4\pi q}\frac{\partial\omega_{01}}{\partial\varepsilon}, \end{aligned} \tag{20}$$

and

$$X = r_{01} \simeq (2qm\omega_{01})^{-1/2}. \tag{21}$$

We omitted the last term of Eq. (18), which is proportional to the identity operator. Here, $\hat{\sigma}_{x,y,z}$ are Pauli operators. The off-diagonal matrix element X is approximated by the value of the harmonic oscillator.

1. Interaction between the classical circuit and the breather qubit

The classical ac $I_{ac}(t)$ is expressed as $I_{ac}(t)=I_{ac}(e^{i\omega t}+e^{-i\omega t})$ with the frequency ω and the amplitude I_{ac}. The interaction Hamiltonian [Eq. (17)] is then represented by using the qubit basis as

$$\begin{aligned} \hat{H}_1 &= \alpha(x_g)(Z\hat{\sigma}_z + X\hat{\sigma}_x)(e^{i\omega t} + e^{-i\omega t}) \\ &\sim \alpha(x_g)X\{\hat{\sigma}_- e^{i\omega t} + \hat{\sigma}_+ e^{-i\omega t}\}, \end{aligned} \tag{22}$$

with $\alpha(x_g)=I_{\mathrm{ac}}I_F dM(x_g)/dx$ and $\hat{\sigma}_\pm=(\hat{\sigma}_x \pm i\hat{\sigma}_y)/2$. Here, we neglected the terms that do not obey the energy conservation rule in the total Hamiltonian of this system, i.e., we used a rotating wave approximation (RWA) under the condition $\hbar\omega \simeq \hbar\omega_{01}$. Equation (22) is then equivalent to that for an atom-field interaction on resonance. Thus, we can perform any unitary operation on a single qubit in the same way as with an NMR qubit. When $\alpha(x_g)$ is assumed to be constant in the interaction range, the state of the breather evolves into

$$|\psi(\tau)\rangle = U(\tau)|\psi(0)\rangle = e^{-i\hat{\sigma}_z\omega\tau}e^{-i\hat{\sigma}_x\Omega_1\tau}|\psi(0)\rangle, \tag{23}$$

after interaction duration τ, where $\Omega_1=\alpha X/\hbar$ is the Rabi frequency. Two factors constitute $U(t)$, namely, the rotating operators $R_z(\theta)=e^{-i\hat{\sigma}_z\theta}$ and $R_x(\theta)=e^{-i\hat{\sigma}_x\theta}$, which rotate around the z and x axes, respectively. By using these rotations, the state vector can move the entire Bloch sphere. Therefore, any one-qubit operation is possible by adjusting the interaction duration τ, namely, the speed of the breather qubit v. For example, a Hadamard transformation[25] is performed by selecting the τ that satisfies two conditions: $\Omega_1\tau=\pi/4+2\pi n$ and $\omega\tau=\pi/2+2\pi m$, where n and m are integers.

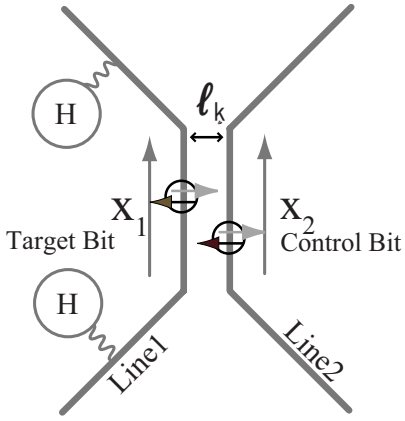

FIG. 6. (Color online) Configuration of our CNOT gate: The target bit is transformed by the Hadamard gate before and after the interaction with the control bit on line 2 separated by length l.

2. Interaction between the quantum circuit and the breather qubit

The interaction between a breather qubit and a quantum LC circuit[26] can also be treated in the same manner with a spin-1/2 particle in a quantized cavity. The current of the quantum LC circuit with resonant frequency ω_{LC} is quantized as

$$\hat{I}_{LC} = \sqrt{\frac{\hbar\omega_{LC}}{2L}}(\hat{a} + \hat{a}^{\dagger}), \tag{24}$$

where $\hat{a}$ ($\hat{a}^{\dagger}$) is the plasmon annihilation (creation) operator and L is the inductance of the quantum LC circuit. In this case, the interaction Hamiltonian is given by

$$\hat{H}_1 = \alpha'(x_g)X(\hat{\sigma}_+\hat{a} + \hat{a}^{\dagger}\hat{\sigma}_-), \tag{25}$$

where $\alpha'(x_g) = I_F\sqrt{\hbar\omega_{LC}/2L}dM(x_g)/dx$.

Suppose that the quantum LC circuit is prepared at the ground state $|0\rangle_{LC}$. If the breather qubit is initially at $|0\rangle$, both the breather qubit and the quantum LC (QLC) states remain unchanged. Otherwise, the qubit state is given at $|0\rangle$, the coupled state evolves as

$$|\phi(\tau)\rangle = \cos\Omega_1'\tau|10\rangle - i\sin\Omega_1'\tau|01\rangle, \tag{26}$$

where $\Omega_1' = \alpha' X/\hbar$ is the Rabi frequency. The coupled state is defined as $|10\rangle = |1\rangle \otimes |0\rangle_{QLC}$, for example. Thus, the QLC at the ground state and the incoming breather qubit at the state $i=0,1$, i.e., the $|i0\rangle$ state, changes to the $|0i\rangle$ state after π-pulse duration. In this way, a breather state is transferred to a stationary QLC state. Thus, the state of a breather qubit can be read out through the QLC state. In the same way, we can introduce the quantum state to the breather qubit via the QLC by reversing the readout processes.

B. Two-qubit operation

Suppose that a target qubit at $x_1 = x_{g1}$ and a control qubit with three energy levels at $x_2 = x_{g2}$ are located in different Josephson lines, as shown in Fig. 6. The third energy state

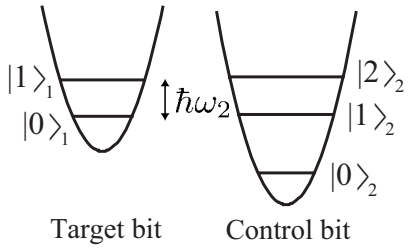

FIG. 7. An energy diagram of a target bit and a control bit. The internal level spacing between $|1\rangle_1$ and $|0\rangle_1$ for the target bit and between $|2\rangle_2$ and $|1\rangle_2$ for the control bit is adjusted to be equal to $\hbar\omega_2$.

$|2\rangle_2$ is used as an auxiliary state to identify whether the control state occupies $|1\rangle$ or not. The interaction Hamiltonian between them is obtained by considering all possible combinations of interactions among fluxons and antifluxons,

$$\begin{aligned} H_2 = \sum_{i,j=F,A} M(x_{i1},x_{j2})I_{i1}I_{j2} = I_{F1}I_{F2}\Bigg[& M\left(x_{g1}+\frac{r_1}{2},x_{g2}+\frac{r_2}{2}\right) \\ & - M\left(x_{g1}+\frac{r_1}{2},x_{g2}-\frac{r_2}{2}\right) - M\left(x_{g1}-\frac{r_1}{2},x_{g2}+\frac{r_2}{2}\right) \\ & + M\left(x_{g1}-\frac{r_1}{2},x_{g2}-\frac{r_2}{2}\right)\Bigg] \simeq I_{F1}I_{F2}\frac{\partial^2 M(x_{g1},x_{g2})}{\partial x_1 \partial x_2} r_1 r_2 \\ \equiv \beta(x_{g1},x_{g2})r_1 r_2, & \end{aligned} \tag{27}$$

where I_{Fi} ($I_{Ai} = -I_{Fi}$) is the current of the fluxon (the antifluxon) in the breather on the ith line. $M(x_1,x_2)$ is the mutual inductance between fluxons in lines 1 and 2. The coordinates of the fluxon and antifluxon in the ith breather are denoted by $x_{F(A)i} = x_{g1(2)} + (-)r_i/2$.

Since $\beta(x_{g1},x_{g2})$ decreases rapidly as the distance between the breathers increases, the interaction between the breathers is turned on only when the breathers are in parallel lines, as shown in Fig. 6. The coupling $\beta(x_{g1},x_{g2})$ becomes constant when two lines are parallel, and the breathers move at the same speed because $\beta(x_{g1},x_{g2})$ depends only on the relative coordinate of the breathers. In the same manner as Eq. (22), the collective-coordinate operators $\hat{r}_1$ and $\hat{r}_2$ can be expanded by the eigenstates $|n\rangle_i$ of each Hamiltonian of the breathers on the ith line as

$$\hat{H}_2 = \beta\hat{r}_1\hat{r}_2 \simeq \beta Z_1 Z_2' \hat{\sigma}_z^{(1)}\hat{\sigma}_z^{(2)} + \beta X_1 X_2'(\hat{\sigma}_+^{(1)}\hat{\sigma}_-^{(2)} + \hat{\sigma}_+^{(2)}\hat{\sigma}_-^{(1)}), \tag{28}$$

where the operators $\hat{\sigma}_-^{(1)}$ and $\hat{\sigma}_-^{(2)}$ are defined as $\hat{\sigma}_-^{(1)} = |0\rangle\langle 1|_1$ and $\hat{\sigma}_-^{(2)} = |1\rangle\langle 2|_2$, respectively. Note that the control bit has three levels, and $\hat{r}_2$ is expanded in the upper two levels: $|1\rangle_2$ and $|2\rangle_2$. Thus, Z' and X' denote the expansion coefficients in these bases. The RWA is also used under the condition shown in Fig. 7. This Hamiltonian induces entangled quantum oscillations between two breathers.

When the control bit is in the $|0\rangle$ state, the two-qubit state does not evolve in the RWA. Otherwise, the two-qubit state changes to

$$|01\rangle \to e^{-i\beta ZZ'/\hbar\tau}|01\rangle, \tag{29}$$

$$|11\rangle \to e^{i\beta ZZ'/\hbar\tau}(\cos\Omega_2\tau|11\rangle - i\sin\Omega_2\tau|02\rangle), \tag{30}$$

after the interaction duration τ, where $\hbar\Omega_2 \equiv \beta X_1 X_2'$. With a π-pulse condition ($\Omega_2\tau=\pi$), the time translation operator on a two-bit basis becomes a controlled-$R_z(\theta)$ gate with $\theta=[1+2(ZZ'/XX')]\pi$. These coefficients are numerically calculated in a two-state situation, $\varepsilon=0.97$ as $Z=0.028$, $X=0.15$. This gate becomes a controlled-σ_z (CZ) gate if we neglect the extra factor $2(ZZ'/XX')\sim 2(Z/X)^2=0.07$. It is well known that a CNOT gate can be constructed by using a CZ gate and Hadamard gates.[25] Therefore, a CNOT gate can be constructed with the gate configuration, as shown in Fig. 6. Note that a CNOT gate can also be constructed by using any two-qubit phase gate, even if we take the extra phase into consideration. This gate is also universal.[27]

IV. DECOHERENCE

In this section, we consider the effect of the fluctuating bias current on the decoherence time of a breather qubit. Fluctuations have two main origins: (i) the dissipative tunneling of quasiparticles across the junction and (ii) intrinsic noise in the current source. In a large junction, the fluctuating bias current from external noise decreases as the junction area increases. So, we study the decoherence caused by the fluctuation originating from dissipative quasiparticle tunneling, which is represented as $\alpha\phi_t$ in Eq. (1).

It is well known that Eq. (1) is not derived from a Lagrangian formalism when $\alpha\neq 0$. Let us include the dissipative effect in the collective-coordinate approach. We multiply the partial differential with respect to r of the ansatz function of Eq. (5) by both sides of Eq. (1) and integrate over the whole space,[28]

$$\int_{-\infty}^{\infty} dx\left(\frac{\partial\phi}{\partial r}\right)(\phi_{tt}-\phi_{xx}+\sin\phi-\varepsilon) = \int_{-\infty}^{\infty} dx\left(\frac{\partial\phi}{\partial r}\right)(-\alpha\phi_t). \tag{31}$$

The left hand side of this equation is rewritten as

$$\int_{-\infty}^{\infty} dx\left(\frac{\partial\phi}{\partial r}\right)\left[\frac{\partial}{\partial t}\frac{\partial\mathcal{L}}{\partial\phi_t}+\frac{\partial}{\partial x}\frac{\partial\mathcal{L}}{\partial\phi_x}-\frac{\partial\mathcal{L}}{\partial\phi}\right]. \tag{32}$$

Then, using the identity,

$$\frac{\partial\phi_t}{\partial\dot{r}} = \frac{\partial\phi}{\partial r}, \tag{33}$$

and provided that

$$\frac{\partial\phi}{\partial r}\frac{\partial\mathcal{L}}{\partial\phi_x}\bigg|_{x=\infty} - \frac{\partial\phi}{\partial r}\frac{\partial\mathcal{L}}{\partial\phi_x}\bigg|_{x=-\infty} = 0, \tag{34}$$

Eq. (32) yields

$$\frac{d}{dt}\left(\frac{\partial L}{\partial\dot{r}}\right)-\frac{\partial L}{\partial r}. \tag{35}$$

On the other hand, the right hand side of Eq. (31) becomes

$$-\alpha m(r)\dot{r}. \tag{36}$$

As a result, the classical equation of motion for r under dissipative forces is given as follows:

$$\frac{d}{dt}\left(\frac{\partial L}{\partial\dot{r}}\right)-\frac{\partial L}{\partial r} = -\alpha m(r)E_J\dot{r}. \tag{37}$$

Hereafter, we neglect the r dependence of the particle mass $m(r)$ since the variation of r in the highly tilted potential is small.

The dissipative term in Eq. (37) stems from the inevitable interaction with the system and the environment. We employ the phenomenological model successfully introduced by Caldeira and Leggett, in order to describe dissipation in quantum mechanics.[29] In their theory, the total Hamiltonian $\hat{H}_{tot}$ is written as

$$\hat{H}_{tot} = \hat{H} + \hat{H}_{env} + \hat{H}_{int}. \tag{38}$$

The system Hamiltonian $\hat{H}$ describes the quantum system of interest, i.e., the bare breather. The second term $\hat{H}_{env}$ is the Hamiltonian of the environment modeled by a set consisting of a huge number of harmonic oscillators with generalized momenta $\hat{p}_\alpha$ and coordinates $\hat{x}_\alpha$,

$$\hat{H}_{env} = \sum_\alpha\left(\frac{\hat{p}_\alpha^2}{2m_\alpha}+\frac{m_\alpha\omega_\alpha^2}{2}\hat{x}_\alpha^2\right), \tag{39}$$

where m_α and ω_α are masses and oscillator frequencies, respectively. The third term $\hat{H}_{int}$ is the coupling between the breather and the environment,

$$\hat{H}_{int} = -2\pi E_J\delta\hat{\varepsilon}\otimes\hat{r}+\Delta U(\hat{r}), \tag{40}$$

where the fluctuating current operator $\delta\hat{\varepsilon}$ holds the relation $2\pi E_J\delta\hat{\varepsilon}=\Sigma_\alpha c_\alpha\hat{x}_\alpha$ and c_α are coupling parameters. This interaction reproduces the dissipative term in a classical equation of motion [Eq. (37)] when the spectral density is Ohmic,

$$J(\omega) \equiv \frac{\pi}{2\hbar}\sum_\alpha\frac{c_\alpha^2}{m_\alpha\omega_\alpha}\delta(\omega-\omega_\alpha) = \alpha mq\omega. \tag{41}$$

The term $\Delta U(\hat{r})=\Sigma_\alpha c_\alpha^2\hat{r}^2/2m_\alpha\omega_\alpha^2$ compensates for the energy renormalization caused by the system-environment interaction. In a highly biased case, the total Hamiltonian $\hat{H}_{tot}$ is reduced to a spin-boson Hamiltonian,

$$\hat{H}_{tot} = \frac{\hbar\omega_{01}}{2}\hat{\sigma}_z - 2\pi E_J\delta\hat{\varepsilon}\otimes(Z\hat{\sigma}_z+X\hat{\sigma}_x)+\hat{H}_{env}. \tag{42}$$

Coupling proportional to $\hat{\sigma}_x$ induces longitudinal relaxation, which means energy relaxation from system to environment. Another coupling proportional to $\hat{\sigma}_z$ causes a random phase shift and dephasing as follows. The longitudinal relaxation time T_1 and the transverse relaxation time T_2 were originally evaluated for the spin-boson model by using a path-integral technique.[29,30] For the relaxation time T_1, the dephasing time T_2, and the pure dephasing time T_ϕ, the Caldeira-Leggett theory gives

$$T_1^{-1} = \left. \frac{X^2}{2} J(\omega) \coth \frac{\hbar\omega}{2kT} \right|_{\omega=\omega_{01}}, \tag{43}$$

$$T_2^{-1} = \frac{1}{2T_1} + \frac{1}{T_\phi}, \tag{44}$$

$$T_\phi^{-1} = \left. \frac{Z^2}{2} J(\omega) \coth \frac{\hbar\omega}{2kT} \right|_{\omega\to 0}, \tag{45}$$

where k and T are Boltzmann's constant and temperature, respectively. Using the $J(\omega)=\alpha m q \omega$ and expressions of components Z and X, Eqs. (20) and (21) are given as

$$T_1^{-1} = \frac{\alpha\omega_J}{4} \tanh \frac{\hbar\omega_{01}}{2kT}, \tag{46}$$

$$T_\phi^{-1} = \frac{\alpha m}{16\pi^2 q} \frac{kT}{\hbar}. \tag{47}$$

Using temperature dependence of the quasiparticle resistance $R(T)$ below the superconducting transition temperature,

$$R(T) = R_n e^{\Delta(T)/kT}. \tag{48}$$

The temperature dependence of the parameter α is then given as[31]

$$\alpha(T) = \frac{1}{\omega_J C R_n} e^{-\Delta(T)/kT}, \tag{49}$$

where R_n and $\Delta(T)$ are the normal resistance associated with the tunnel barrier and superconducting gap energy, respectively.

Using experimental values for a $10\times 10\ \mu\text{m}^2$ NbN/MgO/NbN junction, the parameters are $R_n=5.33\ \Omega$, $C=7.5\times 10^{-12}$ F, and $\Delta=2.5$ meV=29 K.[21] We obtain $T_1=95\ \mu$s and $T_\phi=2.8$ ms even at $T=2.3$ K. These suggest that any decoherence caused by quasiparticles is negligible at lower temperatures. The other mechanisms that we disregarded, such as quasiparticle-phonon interaction, will be considered elsewhere.

V. IMPLEMENTATION

Finally, let us roughly estimate some parameters by using plausible experimental values.

Estimation for one-bit operation. We estimate the breather velocity $v_{a\pi}$ required for an $a\pi$-gate operation; $\Omega_1\tau=a\pi$. Since $dM/dx \simeq M/v_{a\pi}\tau$, the operation relation yields

$$\Omega_1\tau = \frac{I_{ac}I_F X\lambda_J}{\hbar}\frac{M}{v_{a\pi}} \simeq \frac{I_{ac}I_F X\lambda_J}{\hbar}\frac{\mu S}{4\pi l_1^3 v_{a\pi}}\pi\lambda_J^2 = a\pi, \tag{50}$$

where the mutual inductance M is estimated by regarding the ac circuit as a magnetic dipole $M \simeq \pi\lambda_J^2 B(0)/I_{ac} = \pi\lambda_J^2\mu S/4\pi l_1^3$. The parameters S and l_1 are the area of the ac circuit and the distance between the circuit and the junction, respectively. Thus, we obtain

$$v_{a\pi} = \frac{I_{ac}I_F X}{\hbar}\frac{\mu S}{4\pi l_1^3 a\pi}\pi\lambda_J^3. \tag{51}$$

From this relation, we finally obtain the relation $v_{a\pi}=v_\pi/a = 0.05\bar{c}/a$ with $\bar{c}$ being the Swihart velocity, which is calculated as 1% of the light speed in a vacuum $\bar{c}=0.01c$ where $I_{ac}=10^{-4}A$ and $l_1=5.0\times 10^{-5}$ m, when $S=10^{-11}$ m^2 and $\lambda_J = 6.0\ \mu$m.

Estimation for two-bit operation. We evaluate the coupling constant of the breather-breather interaction. The magnetic dipole on one line produces a magnetic flux density on the other line with the separation l_2. The magnetic field density is expressed as

$$B(x_{g1}-x_{g2}) = \frac{\mu\pi\lambda_J^2 I_F}{4\pi\{(x_{g1}-x_{g2})^2 + l_2^2\}^{3/2}}. \tag{52}$$

Then, the derivative of mutual inductance $[M=B(x_{g1}-x_{g2})\pi\lambda_J^2/I_F]$ is expressed as $\partial^2 M/\partial x_1\partial x_2|_{x_{g1}=x_{g2}} = 3\pi\mu\lambda_J^4/4l_2^5$. Therefore, the Rabi frequency is given as $\Omega_2 = \beta X_1 X_2'/\hbar \simeq I^2X^2(\partial^2 M/\partial x_1\partial x_2)\lambda_J^2/\hbar$ and is estimated as $2.2\times 10^{-11}/l_2^5$ s^{-1}. When $l_2=4.5\times 10^{-5}$ m, $\Omega_2=2.7\times 10^{10}$ s^{-1} and therefore, the π-pulse line length $l_\pi=\pi v/\Omega_2$ is 5.7 μm.

VI. SUMMARY

In summary, we have proposed a type of flux qubit, i.e., the mobile qubit, using elementary excitations in superconducting solid-state quantum circuits, which can be introduced anytime and anywhere "on demand" into quantum networks. Our proposed mobile qubit can solve the unavoidable problem concerning the coherent manipulation of the interaction between an arbitrary pair of stationary qubits built in solid-state quantum circuits. Moreover, it can interact with the other breather qubit stronger than the optical qubit, so it can realize more reliable two-qubit gates. In addition, the interaction time of our qubits can be controlled by controlling the speed. This is unlike optical qubits where the degree of phase shift cannot be controlled once the gate arrangement has been designed. Our qubit can also contribute to quantum-information transfer from one place to another by acting as a quantum data bus that can help to construct clusters of quantum computers. Our mobile qubits can form the quantum logic gates required for quantum-information processing without any help from conventional stationary qubits. Therefore, our mobile breather qubits can integrate quantum computation and communication in the same system.

We have also estimated the longitudinal relaxation time T_1 and pure dephasing time T_ϕ by using the spin-boson model and obtained $T_1\sim 95\ \mu$s and $T_\phi\sim 2.8$ ms at 2.3 K. These values are comparable to the T_1 and T_ϕ values of the other types of Josephson qubit at very low temperatures such as 25 mK.[32] This suggests that our qubit may also be a possible candidate for a quantum computer.

In addition, our mobile breather qubit can provide a platform for testing fundamental problems in quantum mechanics on a macroscopic scale, such as macroscopic Bell's pair experiments in both the space and time domains, since it can be regarded as a macroscopic object produced by a huge number of coherent Cooper pairs. This will be an important goal in the next generation of experiments designed to definitively rule out the alternative hypothesis of macrorealism.

ACKNOWLEDGMENTS

We would like to thank A. Ustinov, S. Tanda, S. Kawabata, M. Iinuma, and D. Meacock for valuable discussions. This work was supported in part by a Grant-in-Aid for Scientific Research (18540352, 17740267, and 195836) from the Ministry of Education Culture, Sports, Science and Technology of Japan.

[1] Q. A. Turchette, C. J. Hood, W. Lange, H. Mabuchi, and H. J. Kimble, Phys. Rev. Lett. **75**, 4710 (1995).
[2] C. Monroe, D. M. Meekhof, B. E. King, W. M. Itano, and D. J. Wineland, Phys. Rev. Lett. **75**, 4714 (1995).
[3] N. A. Gershenfeld and I. L. Chuang, Science **275**, 350 (1997).
[4] Y. Yu, S. Han, X. Chu, S.-I. Chu, and Z. Wang, Science **296**, 889 (2002).
[5] D. Vion, A. Aassime, A. Cottet, P. Joyez, H. Pothier, C. Urbina, D. Esteve, and M. H. Devoret, Science **296**, 886 (2002).
[6] D. V. Averin and C. Bruder, Phys. Rev. Lett. **91**, 057003 (2003).
[7] B. L. T. Plourde, J. Zhang, K. B. Whaley, F. K. Wilhelm, T. L. Robertson, T. Hime, S. Linzen, P. A. Reichardt, C. E. Wu, and J. Clarke, Phys. Rev. B **70**, 140501(R) (2004).
[8] I. L. Chuang and Y. Yamamoto, Phys. Rev. A **52**, 3489 (1995).
[9] P. Domokos, J. M. Raimond, M. Brune, and S. Haroche, Phys. Rev. A **52**, 3554 (1995).
[10] W. Anacker, IBM J. Res. Dev. **24**, 107 (1980).
[11] H. H. Zappe, Appl. Phys. Lett. **25**, 424 (1974).
[12] A. Shnirman, Z. Hermon, L. Vaidman, and E. Ben-Jacob, Phys. Rev. A **52**, 3541 (1995).
[13] T. Kato and M. Imada, J. Phys. Soc. Jpn. **65**, 2963 (1996).
[14] A. Shnirman, E. Ben-Jacob, and B. Malomed, Phys. Rev. B **56**, 14677 (1997).
[15] A. Wallraff, A. Lukashenko, J. Lisenfeld, A. Kemp, M. V. Fistul, Y. Koval, and A. V. Ustinov, Nature (London) **425**, 155 (2003).
[16] M. V. Fistul, A. Wallraff, Y. Koval, A. Lukashenko, B. A. Malomed, and A. V. Ustinov, Phys. Rev. Lett. **91**, 257004 (2003).
[17] A. Wallraff, Y. Koval, M. Levitchev, M. V. Fistul, and A. V. Ustinov, J. Low Temp. Phys. **118**, 543 (2000).
[18] R. Rajaraman, *Solitons and Instantons: An Introduction to Solitons and Instantons in Quantum Field Theory* (North-Holland, Amsterdam, 1987).
[19] R. F. Dashen, B. Hasslacher, and A. Neveu, Phys. Rev. D **11**, 3424 (1975).
[20] K. Maki and H. Takayama, Phys. Rev. B **20**, 5002 (1979).
[21] A. Shoji, M. Aoyagi, S. Kosaka, F. Shinoki, and H. Hayakawa, Appl. Phys. Lett. **46**, 1098 (1985).
[22] M. Wintersgill and J. Fontanella, J. Appl. Phys. **50**, 8259 (1979).
[23] O. Legrand and G. Reinisch, Phys. Rev. A **35**, 3522 (1987); C. D. Ferguson and C. R. Willis, Physica D **119**, 283 (1998).
[24] T. Matsuda, Lett. Nuovo Cimento Soc. Ital. Fis. **24**, 207 (1979).
[25] G. Benenti, G. Casati, and G. Strini, *Principles of Quantum Computation and Information* (World Scientific, Singapore, 2004).
[26] J. Johansson, S. Saito, T. Meno, H. Nakano, M. Ueda, K. Semba, and H. Takayanagi, Phys. Rev. Lett. **96**, 127006 (2006).
[27] M. J. Bremner, C. M. Dawson, J. L. Dodd, A. Gilchrist, A. W. Harrow, D. Mortimer, M. A. Nielsen, and T. J. Osborne, Phys. Rev. Lett. **89**, 247902 (2002).
[28] O. Legrand, Phys. Rev. A **36**, 5068 (1987).
[29] A. O. Caldeira and A. J. Leggett, Phys. Rev. Lett. **46**, 211 (1981).
[30] U. Weiss, *Quantum Dissipative Systems*, 2nd ed. (World Scientific, Singapore, 1999).
[31] N. F. Pedersen and D. Welner, Phys. Rev. B **29**, 2551 (1984).
[32] J. Q. You and F. Nori, Phys. Today **58**(11), 42 (2005).